Received: 14 May 2020 | Revised: 1 July 2020 | Accepted: 11 July 2020

DOI: 10.1111/adb.12947

ORIGINAL ARTICLE

Addiction Biology SSA WILEY

Cocaine memory reactivation induces functional adaptations within parvalbumin interneurons in the rat medial prefrontal cortex

Emily T. Jorgensen[1,2] | Angela E. Gonzalez[3,4] | John H. Harkness[3] | Deborah M. Hegarty[5] | Amit Thakar[1,2] | Delta J. Burchi[2] | Jake A. Aadland[2] | Sue A. Aicher[5] | Barbara A. Sorg[3,4] | Travis E. Brown[1,2]

[1]Neuroscience Graduate Program, University of Wyoming, Laramie, Wyoming, USA

[2]School of Pharmacy, University of Wyoming, Laramie, Wyoming, USA

[3]Department of Integrative Physiology and Neuroscience, Translational Addiction Research Center, Washington State University, Vancouver, Washington, USA

[4]R.S. Dow Neurobiology, Legacy Research Institute, Portland, Oregon, USA

[5]Department of Chemical Physiology and Biochemistry, Oregon Health & Science University, Portland, Oregon, USA

Correspondence
Travis E. Brown, University of Wyoming, 1000 E University Ave., Dept 3375, Laramie, WY 82071, USA.
Email: tbrown53@uwyo.edu

Funding information
University of Wyoming Science Initiative; Wyoming Scholars Program; National Institute of Neurological Disorders and Stroke, Grant/Award Number: P30 NS061800; National Institutes of Health Centers Program, Grant/Award Number: P30 GM103398-32128; National Institute on Drug Abuse, Grant/Award Number: R01 DA040965

Abstract

Substance use disorder is a complex disease created in part by maladaptive learning and memory mechanisms following repeated drug use. Exposure to drug-associated stimuli engages prefrontal cortex circuits, and dysfunction of the medial prefrontal cortex (mPFC) is thought to underlie drug-seeking behaviors. Growing evidence supports a role for parvalbumin containing fast-spiking interneurons (FSI) in modulating prefrontal cortical microcircuit activity by influencing the balance of excitation and inhibition, which can influence learning and memory processes. Most parvalbumin FSIs within layer V of the prelimbic mPFC are surrounded by specialized extracellular matrix structures called perineuronal nets (PNN). Previous work by our group found that cocaine exposure altered PNN-surrounded FSI function, and pharmacological removal of PNNs reduced cocaine-seeking behavior. However, the role of FSIs and associated constituents (parvalbumin and PNNs) in cocaine-related memories was not previously explored and is still unknown. Here, we found that reactivation of a cocaine conditioned place preference memory produced changes in cortical PNN-surrounded parvalbumin FSIs, including decreased parvalbumin intensity, increased parvalbumin cell axis diameter, decreased intrinsic excitability, and increased excitatory synaptic input. Further investigation of intrinsic properties revealed changes in the interspike interval, membrane capacitance, and afterhyperpolarization recovery time. Changes in these specific properties suggest an increase in potassium-mediated currents, which was validated with additional electrophysiological analysis. Collectively, our results indicate that cocaine memory reactivation induces functional adaptations in PNN-surrounded parvalbumin neurons, which likely alters cortical output to promote cocaine-seeking behavior.

KEYWORDS

conditioned place preference, electrophysiology, perineuronal nets, potassium, prefrontal cortex, substance use disorder

1 | INTRODUCTION

Repeated drug exposure causes persistent drug-associated memories to form, which can contribute to relapse following abstinence.[1,2] Drug-seeking behaviors can be diminished when the drug-associated memory is weakened or disrupted during the "reconsolidation window," a period of up to 6 h after memory reactivation,[3] when the memory is labile and susceptible to modification.[4–6] Notably, a memory retrieval-extinction procedure has been shown to reduce long-term craving in humans for up to 6 months, which suggests that modifying drug-associated memories through a reconsolidation process is an effective strategy to diminish drug relapse.[6] Relatively few studies have examined the functional neuronal adaptations associated with drug memory reactivation. In this study, we characterized the electrophysiological properties of parvalbumin-containing fast-spiking interneurons (FSIs) and changes in perineuronal net (PNN) and parvalbumin intensity within the medial prefrontal cortex (mPFC) prior to and after cocaine memory reactivation.

Parvalbumin is a high-affinity calcium buffer and is a reliable identifier of GABAergic FSIs within the cortex.[7] Parvalbumin-containing FSIs synapse directly onto layer V pyramidal neurons within the medial PFC and heavily influence excitatory output.[8] Deficits in parvalbumin FSIs have been implicated in multiple disorders of the nervous system, such as schizophrenia.[9,10] Additionally, parvalbumin FSIs are important for behavioral and molecular aspects of learning and memory.[11,12] However, to our knowledge, nothing is known about the role of parvalbumin FSIs in the development and maintenance of drug-associated memories following memory reactivation. In the mPFC, most parvalbumin FSIs are surrounded by PNNs, which we have shown to mediate cocaine-associated memories after reinstatement.[13]

PNNs are specialized extracellular matrix structures composed of chondroitin sulfate proteoglycans, hyaluronin, and other proteins that appear during critical periods of development.[14] Within the PFC, PNNs primarily surround parvalbumin FSIs and broadly contribute to neuronal stability.[15] PNNs serve many functions including protecting underlying neurons from oxidative stress,[16,17] impacting cognitive performance and memory,[18,19] and contributing to the establishment and maintenance of fear memories.[20–22] PNNs are also susceptible to modification following exposure to various substances, including high fat diets[23,24] and cocaine.[13,25] Recent work by us and others has shown that PNN degradation attenuates cocaine-conditioned place preference[26] (cocaine-CPP) and cocaine self-administration.[13,27] However, the relationship between changes in parvalbumin, PNNs, and the functional adaptations in neuronal excitability and synaptic transmission of parvalbumin FSIs within the PFC following cocaine memory reactivation remains unknown.

Our goal was to investigate the functional adaptations in PNN-surrounded FSIs and whether there were corresponding changes in PNNs and parvalbumin following cocaine-CPP memory reactivation. PNNs and parvalbumin are each known to modulate excitability and synaptic communication within the local prefrontal microcircuit and downstream targets,[28,29] and excitatory synaptic plasticity within the neocortex is thought to be important for learning and memory processes.[30] Synaptic plasticity is controlled by many different neuromodulators and generally results in, or is a compensatory response to, a decrease in inhibition (disinhibition), and this disinhibition leads to an altered excitatory:inhibitory balance during periods of learning.[30] Since PNNs and parvalbumin FSIs are implicated in both behavioral and molecular aspects of learning and memory and substance use, we hypothesized that there would be decreased parvalbumin FSI firing and a compensatory response in synaptic transmission and overall increase in the excitatory:inhibitory balance. We speculate these combined circuitry changes are contributing to an increase in cocaine-seeking behaviors. To test our hypothesis, we used behavioral, immunohistochemical, and electrophysiological approaches to identify functional adaptations in PNN-surrounded parvalbumin FSIs following cocaine memory reactivation, a window of plasticity where the cocaine memory is thought to be strengthened.

2 | MATERIALS AND METHODS

2.1 | Animals

All procedures were performed in accordance with the National Institutes of Health's *Guidelines for the Care and Use of Laboratory Animals* and with approval from the Institutional Animal Care and Use Committee at the University of Wyoming and Washington State University. A total of 107 adult male Sprague-Dawley rats was used for these experiments. All rats were bred in house with ad libitum access to food and water and weighed ~300–400 g during the experiment. Rats were housed in a temperature (25°C) and humidity-controlled room maintained on a 12-h light/dark cycle, with lights on at 0700. All efforts were made to minimize the number of animals used in the experiments and to reduce the amount of pain and suffering.

2.2 | Cocaine-conditioned place preference

All cocaine-conditioned place preference (CPP) experiments were conducted during the light phase of the daily light/dark cycle. The CPP apparatus consists of three Plexiglas compartments, including two primary outer chambers (28 × 21 × 21 cm), one with black walls and metal rod floors and the other with white walls and wire mesh floors. The center chamber (12 × 21 × 21 cm) has gray walls with solid gray Plexiglas flooring (Med Associates, Fairfax, VT). Time spent in each chamber was automatically recorded with infrared photocell beams within the apparatus. Manual guillotine doors separate each chamber, confining the rat to one side of the CPP apparatus during conditioning.

Rats received 2 days of 15 min exposure to all three chambers: the first day served as a habituation day, and the second day served as a test for initial preference (Figure 1A for timeline). Time spent within each compartment was recorded. The cocaine-paired chamber was chosen by counterbalancing the preferred and non-preferred sides in

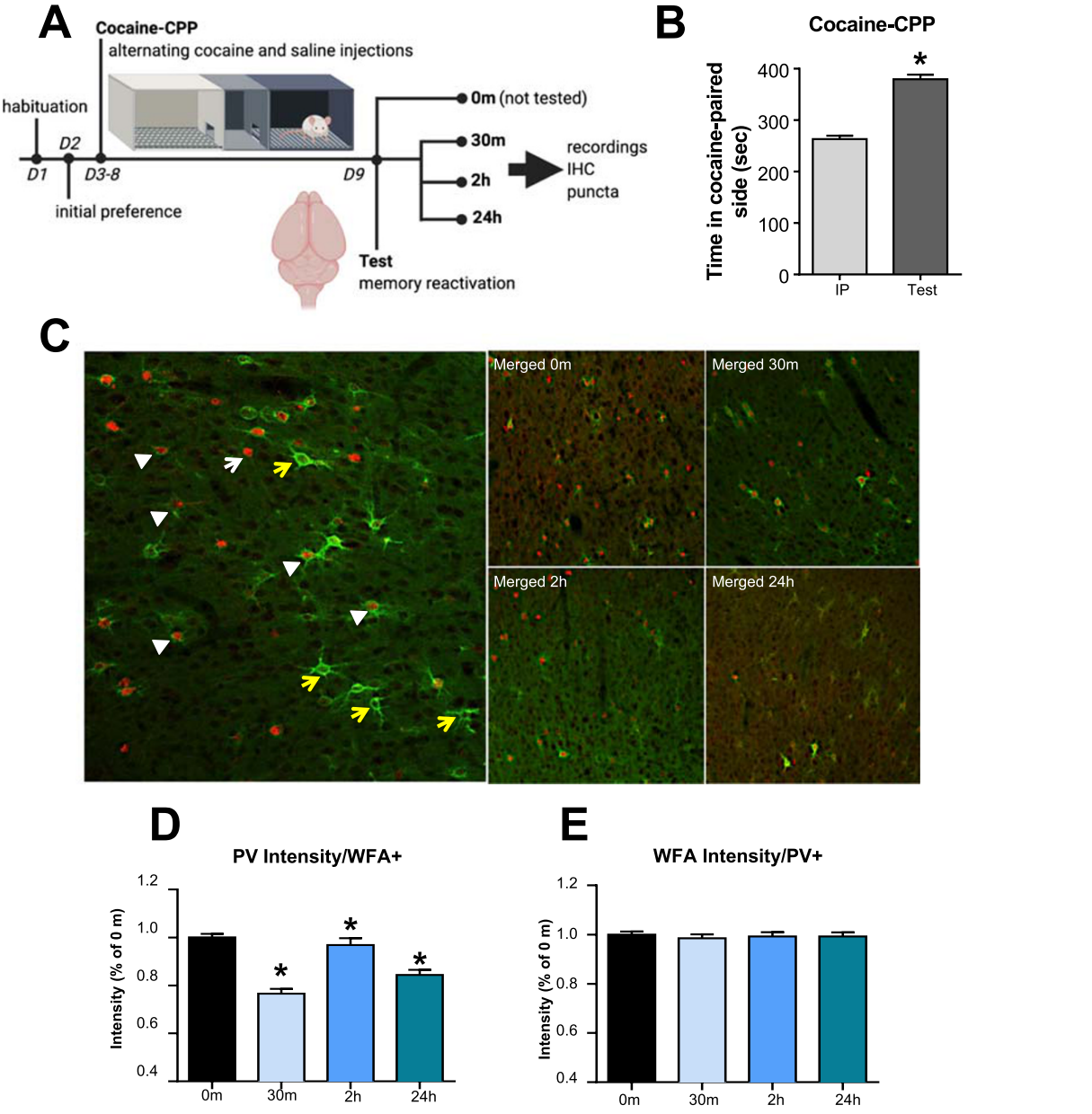

FIGURE 1 Cocaine memory reactivation decreases parvalbumin (PV) intensity in WFA$^+$-surrounded neurons within the PL PFC. (A) Experimental timeline. Fifteen-minute habituation for CPP apparatus; initial preference = 15 min in cocaine-paired chamber prior to training; cocaine CPP = 25 min 12 mg/kg, intraperitoneal (i.p.) cocaine-pairing alternating with 25 min 1 ml/kg i.p. saline-pairing; test for cocaine-paired chamber after cocaine training procedure in which no cocaine was administered; rats were euthanized at indicated timepoints for analysis; (B) time spent in cocaine-paired chamber on initial preference and test day for CPP. Rats conditioned with cocaine (n = 78) show place preference; (C) representative photomicrograph of PV$^+$ cells with (white arrowheads) and without (white arrows) WFA$^+$ perineuronal nets in the prelimbic PFC. We also observed WFA nets around non-PV cells (yellow arrows). Right panels are representative images for each time point. (D) PV intensity in PV cells surrounded by WFA cells was decreased at all time points after cocaine memory reactivation; (E) WFA intensity surrounding PV$^+$ cells was not altered. N-sizes: (t = 0 [12]; t = 30 m [6]; t = 2 h [5]; t = 24 h [7]). $^*p < 0.05$, compared with t = 0 time point

addition to the black and white chambers. Saline and cocaine (gift from National Institute of Drug Abuse) were administered on alternate days for six training days. Each rat received three saline (1 ml/kg, intraperitoneal [i.p.]) and three cocaine (12 mg/kg, i.p.) pairings. Following cocaine or saline injections, each rat was confined to the assigned chamber for 25 min.[13] Following cocaine-CPP training, rats were given a memory reactivation session in a drug-free state 24 h after their last training injection by placing them in the central chamber with access to all chambers for 15 min. Rats that spent more time on the cocaine-paired chamber compared with the initial preference day were considered to have attained a place preference. Animals were euthanized at select times after the memory reactivation session (30 min, 2 h, and 24 h). To ensure we measured an effect of cocaine memory reactivation, and not previous cocaine training, some rats were not given a memory reactivation session but were removed directly from their home cage 24 h following cocaine-CPP training (t = 0 min).

2.3 | Immunohistochemistry and imaging

2.3.1 | WFA and parvalbumin labeling and imaging

For each rat, we analyzed four to six brain slices (eight to 12 hemispheres). The mean number of cells analyzed per animal is indicated in Section 3. PNNs were identified by staining with *Wisteria floribunda* agglutinin (WFA), a plant lectin that binds to the chondroitin sulfate proteoglycan components of the PNNs. Parvalbumin (Sigma-Aldrich, Cat# SAB4200545, RRID AB_2857970) and WFA (Vector Laboratories, Cat# FL-1351, RRID AB_2336875) were stained as previously described.[25,31,32] All images (1.194 pixels/μm) were compiled into summed images using ImageJ macro plug-in Pipsqueak™ (https://labs.wsu.edu/sorg/research-resources/), scaled, and converted into 8-bit, grayscale, tiff files. Pipsqueak™ was run using the "double-label analysis" function in "semi-automatic mode" to select ROIs to identify individual parvalbumin$^+$ cells and PNNs, which were then verified by a trained experimenter who was blinded to the experimental conditions. The plug-in compiles this analysis to identify single[32] and double-labeled neurons[31] (https://ai.RewireNeuro.com).

2.3.2 | Puncta labeling and imaging

Immunohistochemical methods for labeling and visualizing excitatory and inhibitory puncta onto PNN-surrounded parvalbumin neurons and subsequent image analysis were performed as previously described.[25,33,34] PNNs were identified using a biotinylated *Wisteria floribunda* lectin (WFA, Vector Laboratories, Cat# B-1355, RRID: AB_AB_2336874). The primary antibody cocktail contained goat anti-glutamic acid decarboxylase 65/67 (GAD 65/67, Santa Cruz Biotechnology, Cat# sc-7513, RRID:AB_2107745, 1:100), rabbit anti-parvalbumin (Novus Biologicals, Cat# NB120-11427, RRID: AB_791498, 1:1000) and guinea pig anti-vesicular glutamate transporter 1 (VGluT1, EMD Millipore, Cat# AB5905, RRID:AB_2301751, 1:5000). Labeled PNNs were visualized using Alexa Fluor 405-conjugated streptavidin (ThermoFisher Scientific, Cat# S32351, 6.25 μg/ml). Secondary antibodies were diluted 1:800 and included Alexa Fluor 488 donkey anti-goat (ThermoFisher Scientific, Cat# A11055, RRID:AB_2534102), Alexa Fluor 546 donkey anti-rabbit (Thermofisher Scientific, Cat# A10040, RRID:AB_2534016), and Alexa Fluor 647 donkey anti-guinea pig (Jackson ImmunoResearch laboratories, Cat# 706-605-148, RRID:AB_2340476). For each animal, one caudal and one rostral section of prelimbic cortex within bregma +3.5 to +4.2 were chosen, and two high magnification images were taken at each level using a Zeiss LSM 780 confocal microscope with a 63 × 1.4 NA Plan-Apochromat objective (Carl Zeiss MicroImaging, Thornwood, NY; 2 images/level × 2 levels/animal = 4 images/animal). Using Zen software (Carl Zeiss, RRID:SCR_013672), PV neurons within the boundaries of the field of view in each confocal stack were identified and assessed for the presence of a nucleus. The optical slice through the nucleus at which the ellipsoidal minor axis length of each PV neuron reached its maximum was determined and the PV neuron axis diameter was measured; Z-stacks were created around each PV neuron that measured 1.15 μm and were used for puncta apposition analysis (162 PV neurons/12 animals; 13.5 ± 0.7 (SEM) PV neurons analyzed/animal). Image analysis of GABAergic and glutamatergic appositions onto parvalbumin-labeled neurons was performed using Imaris 8.0 software (BitPlane USA, Concord, MA, RRID:SCR_007370) on an offline workstation in the Advanced Light Microscopy Core at Oregon Health & Science University by a blinded observer.[25,33,34] For puncta analysis, the presence of WFA labeling within 1.5 μm of the parvalbumin neuron surface was assessed for each parvalbumin neuron. A parvalbumin neuron was considered to have a PNN if there was any WFA labeling around any part of the parvalbumin neuron surface as seen by the observer. GAD65/67 and VGluT1-labeled puncta within 0.5 μm of the segmented parvalbumin neuron were then assessed separately using the Imaris *Spots* segmentation tool, followed by the *Find Spots Close to Surface Imaris XTension* tool as previously described.[25]

2.4 | Whole-cell patch clamp electrophysiology

For whole-cell patch clamp, tissue preparation and solution compositions were as previously described.[13,25] Following perfusion, rats were decapitated and coronal slices (300 μm) containing the mPFC (3.2–3.7 mm from bregma[35]) were prepared using a vibratome (Leica VT1200S), placed in ice-cold recovery solution, and incubated for at least 1 h in room temperature, in a modified aCSF holding solution prior to recording.[25] Immediately before recording, slices were incubated in holding solution[25] WFA (1 μg/ml) for 5 min to stain for PNNs. CellSens software (Olympus) was used to identify WFA$^+$ (fluorescing) neurons in layers IV and V of the prelimbic mPFC, and later patched (Figure 1D for representation). Pipettes were filled with K-gluconate intracellular solution for intrinsic experiments. K-gluconate composition was (in mM): 120 K-gluconate, 6 KCl, 10 HEPES, 4 ATP-Mg, 0.3 GTP-Na, 0.1 EGTA, and KOH were added to bring pH to ~7.2. Cells were current-clamped at −70 mV and 10 current steps were injected starting at −100 pA and ending at 800 pA. The duration of each recording was no longer than 5 min per cell with each sweep lasting 100 ms. Elicited action potentials were recorded, counted, and analyzed using pClamp10.3. (Clampfit, Axon Instruments, Sunnyvale, CA).

To record miniature inhibitory postsynaptic currents (mIPSCs), the aCSF[25] bath contained 6,7-dinitroquinoxaline-2,3-dione (DNQX; 10 μM), strychnine (1 μM), and tetrodotoxin (1 μM) to block AMPA, glycine receptors, and sodium channels, respectively. Pipettes were filled with CsCl intracellular solution. CsCl solution composition was (in mM) 117 CsCl, 2.8 NaCl, 5 $MgCl_2$, 20 HEPES, 2 Mg^{2+}ATP, 0.3 Na^{2+}GTP, 0.6 EGTA, and sucrose to bring osmolarity to 275–280 mOsm and pH to ~7.25. Miniature excitatory postsynaptic currents (mEPSCs) were recorded in an aCSF containing picrotoxin (100 μM) and tetrodotoxin (1 μM) to block GABA receptors and sodium channels, respectively. Patch pipettes were filled with KCl intracellular solution. KCl solution composition was (in mM) 125 KCL, 2.8 NaCl, 2 $MgCl_2$, 2 ATP-Na^+, 0.3 GTP-Li^+, 0.6 EGTA, and 10 HEPES.

Cells were voltage-clamped at −70 mV, and input resistance and series resistance were monitored throughout experiments. Miniature recordings were 3 min long with 1 min per sweep. Only one sweep per cell was used for data analysis. Criteria were met if the cell's access resistance was below 30 MΩ. mIPSCs and mEPSCs were amplified and recorded using pClamp10.3, and Mini Analysis Program (Synaptosoft Inc, GA, USA) was used to measure miniature amplitudes and frequencies.

For potassium current isolation experiments, the aCSF contained tetrodotoxin (1 μM) to block sodium channels. Patch pipettes were filled with K-gluconate intracellular solution as described above. Step protocols were replicated from methods previously described.[36] Briefly, cells were voltage clamped at −70 mV and stepped up to +90 mV by increments of 10 mV.

2.5 | Analysis

All statistical tests were conducted using Prism 8 (GraphPad Software). For behavioral experiments, we compared the initial preference and post-training test using a paired *t* test. For intrinsic electrophysiological analysis and potassium recordings, data were analyzed with a two-way, repeated-measures ANOVA followed by a Dunnett's multiple comparison test to compare significance from non-reactivation (*t* = 0 min). For intrinsic properties, data were analyzed with a one-way ANOVA followed by a Tukey's multiple comparison test to compare significance from *t* = 0. For miniature electrophysiological analysis, data were analyzed with a Kolmogorov–Smirnov test when assessing cumulative probability distributions and a one-way ANOVA followed by a Tukey's multiple comparison test when assessing average miniature data. For WFA and parvalbumin intensity, control group mean cell intensities (*t* = 0 min) were used to calculate normalized intensities for each label. Distributions of normalized intensities were then compared between experimental groups, within stain type, using a Kruskal-Wallis test followed by a Dunn's multiple comparison test to assess changes in the distribution of intensities among groups. Comparison among treatment groups for the number of parvalbumin and WFA labeled cells was done using a one-way ANOVA. For puncta analysis, data were analyzed using a Kruskal-Wallis test followed by a Dunn's multiple comparison test. All results are summarized as mean ± standard error of the mean (SEM). Differences were considered significant if $p < 0.05$. The data that support the findings of this study are available upon request from the corresponding author.

3 | RESULTS

3.1 | Cocaine-conditioned place preference alters intensity of parvalbumin in mPFC neurons

Figure 1A shows the experimental timeline. There was a significant increase in place preference for the cocaine-paired chamber during the drug-free CPP test (Figure 1B, test/memory reactivation session) compared with the initial preference (IP) day in all rats (IP = 266 ± 7 s, test = 383 ± 10 s; $t_{77} = 10.48$, $p < 0.0001$). There were no significant differences in CPP between experimental groups (rats used for electrophysiology, immunohistochemistry, or puncta analysis); hence, behavioral data were pooled.

Brains were examined for parvalbumin and WFA staining intensity before (0 min) and 30 min, 2 h, and 24 h after memory reactivation. Figure 1C provides representative images for each time point. Figure 1D shows that the intensity of parvalbumin in WFA-surrounded cells was decreased at all time points (30 min, 2 h, and 24 h) compared with non-reactivated controls ($p < 0.0001$ for all groups; $H = 2.96$). There was no significant difference in the intensity of WFA around parvalbumin cells after reactivation (Figure 1E). There was also no difference in the number of parvalbumin/WFA double-labeled neurons across time points (0 min = 16.9 ± 1.1; 30 min = 21.0 ± 1.6; 2 h = 19.0 ± 2.7; 24 h = 18.8 ± 2.8 cells; $p < 0.438$). We also did not observe any significant correlations between CPP behavior on the test day and either PV or WFA staining intensity (not shown).

3.2 | Cocaine-conditioned place preference increases VGluT1 and axis diameter of parvalbumin mPFC neurons

We examined excitatory and inhibitory puncta apposing parvalbumin cells that were surrounded by PNNs at 2 and 24 h after memory reactivation. The confocal micrograph in Figure 2A and rendering in Figure 2B show a representative parvalbumin neuron surrounded by a WFA-labeled PNN, which receives appositions from glutamatergic (VGluT1, magenta) and GABAergic (GAD 65/67, green) puncta. The number of GAD 65/67 puncta did not change after memory reactivation (Figure 2C), while the number of VGluT1 puncta increased 24 h after memory reactivation compared with *t* = 0 (Figure 2D; $p < 0.01$; $H = 11.05$). The increase in VGluT1 and the slight but nonsignificant decrease in GAD 65/67 led to a decrease in the GAD 65/67: VGluT1 ratio at 24 h compared with *t* = 0 (Figure 2E; $p < 0.05$; $H = 7.44$). Figure 2F shows an increase in parvalbumin cell diameter at both 2 and 24 h following cocaine memory reactivation when compared with *t* = 0 ($p < 0.0001$ for both groups; $H = 31.48$).

3.3 | Cocaine memory reactivation alters excitability and potassium current of PNN-surrounded FSIs

Memory reactivation attenuated the number of current-induced action potentials in WFA^+ (PNN-surrounded) FSIs compared with the non-reactivated controls (*t* = 0) at 30 min and 2 h, and this returned to control levels by 24 h (Figure 3L; reactivation time points: $F_{3,54} = 6.69$, $p < 0.01$; current step: $F_{9,486} = 568.6$, $p < 0.01$; interaction: $F_{27,486} = 3.98$, $p < 0.01$). Some intrinsic properties were increased, including membrane capacitance, the first ISI, and afterhyperpolarization (AHP) duration. Membrane capacitance was

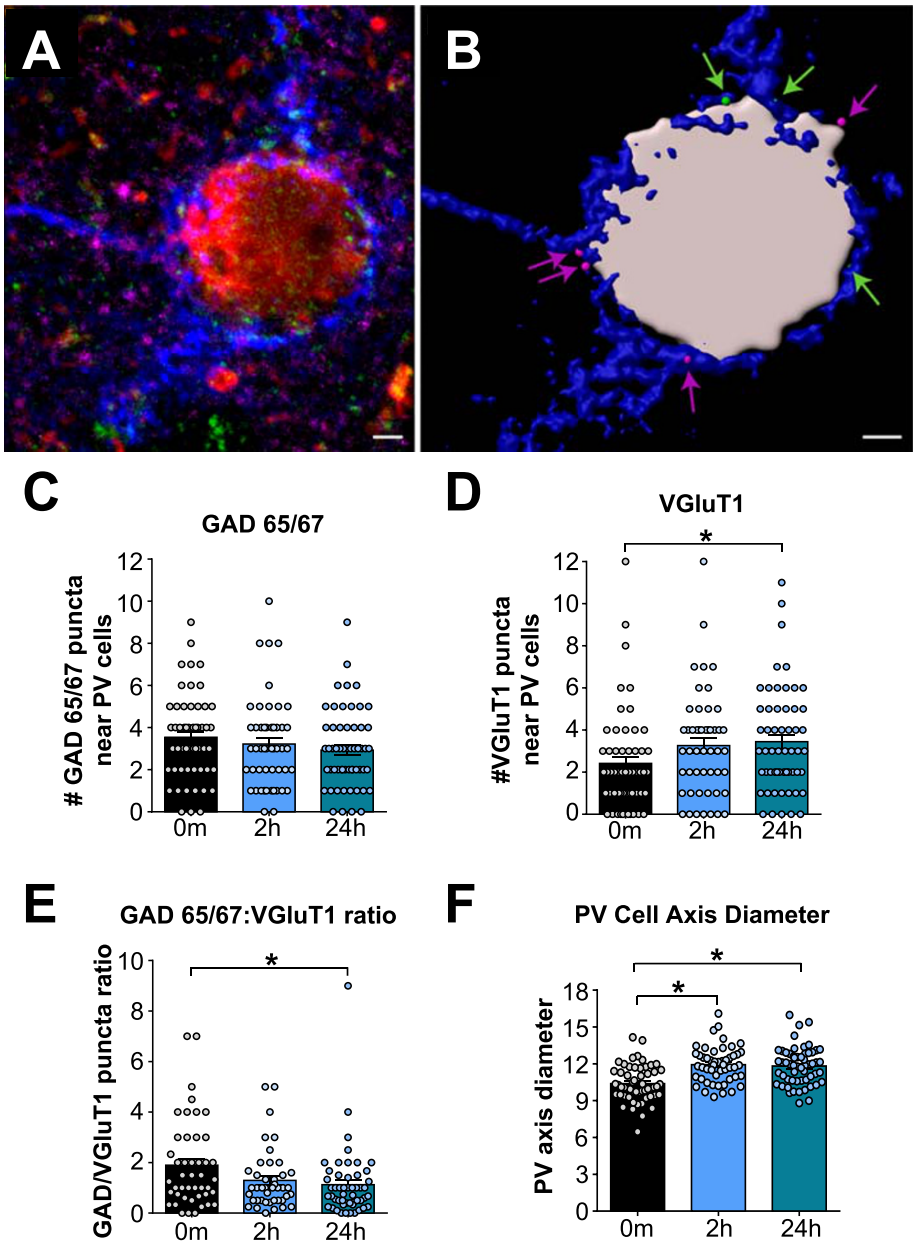

FIGURE 2 Cocaine memory reactivation increases intensity of glutamatergic (VGluT1) puncta near PNN-surrounded parvalbumin neurons and increases PV cell axis diameter. Neurons were visualized with confocal microscopy and analyzed using Imaris segmentation tools. (A) Representative confocal micrograph of a PV neuron (red) surrounded by a PNN labeled with WFA (blue) and receiving appositions from glutamatergic (VGluT1, magenta) and GABAergic (GAD65/67, green) puncta. (B) The PV neuron (gray) and WFA-labeled PNN (blue) were rendered using the Imaris surfaces segmentation tool. GAD65/67 (green arrows) and VGluT1 puncta (magenta arrows) meeting our size and location criteria were segmented using the Imaris spots tool and included in the analysis. Scale bar = 2 μm. (C) GAD 65/67 puncta at t = 0 and 2 and 24 h later; (D) VGluT1 puncta at t = 0 and 2 and 24 h later; (E) the ratio of GAD65/67:VGluT1 at t = 0 and 2 and 24 h later; (F) axis diameter of PV/WFA cells at t = 0 and 2 and 24 h later. N = 4/group. $^{*}p < 0.05$, compared with t = 0 time point

greater 30 min and 2 h following memory reactivation compared with t = 0 (Figure 3D; $F_{3,54}$ = 10.01, $p < 0.01$). ISI was increased at 30 min (Figure 3E; $F_{3,54}$ = 7.98, $p < 0.01$), and AHP duration, or the time it took to repolarize to firing threshold, was increased at 2 h (Figure 3K; $F_{3,54}$ = 4.65, $p < 0.01$). Memory reactivation also induced an increase in the amount of potassium-mediated current at 30 min and 2 h when normalized to membrane capacitance (Figure 3M; reactivation time points: $F_{3,40}$ = 3.91, $p < 0.0001$; current step: $F_{19,760}$ = 261, $p < 0.0001$; interaction: $F_{57,760}$ = 3.63, $p < 0.0001$). However, when normalized to each cell's maximum amount of current, there were no significant differences (Figure 3N). Figure 3O provides representative traces of recorded potassium current. Although traces appear to exhibit different kinetics, tau was measured (point 1 to point 2), and no significant differences were identified (data not shown).

3.4 | Cocaine memory reactivation alters synaptic transmission onto FSIs

Memory reactivation increased average mEPSC frequencies 30 min, 2 h, and 24 h after memory reactivation compared to non-reactivated controls (Figure 4A; 0 min = 0.84 Hz, 30 min = 4.06 Hz, 2 h = 2.67 Hz, and 24 h = 3.38 Hz; $F_{3,77}$ = 10.04, $p < 0.01$). The average miniature data represent collapsed events for each cell to get a sense of individual cell variability. We also provide cumulative data of all the miniature events; this is more sensitive and representative of all miniature events. Hence, we can detect significance in the cumulative plots that are trends when the data were collapsed to the average data. Both are informative as the collapsed data represent animal variability, while the cumulative data give insight into the total event variability.

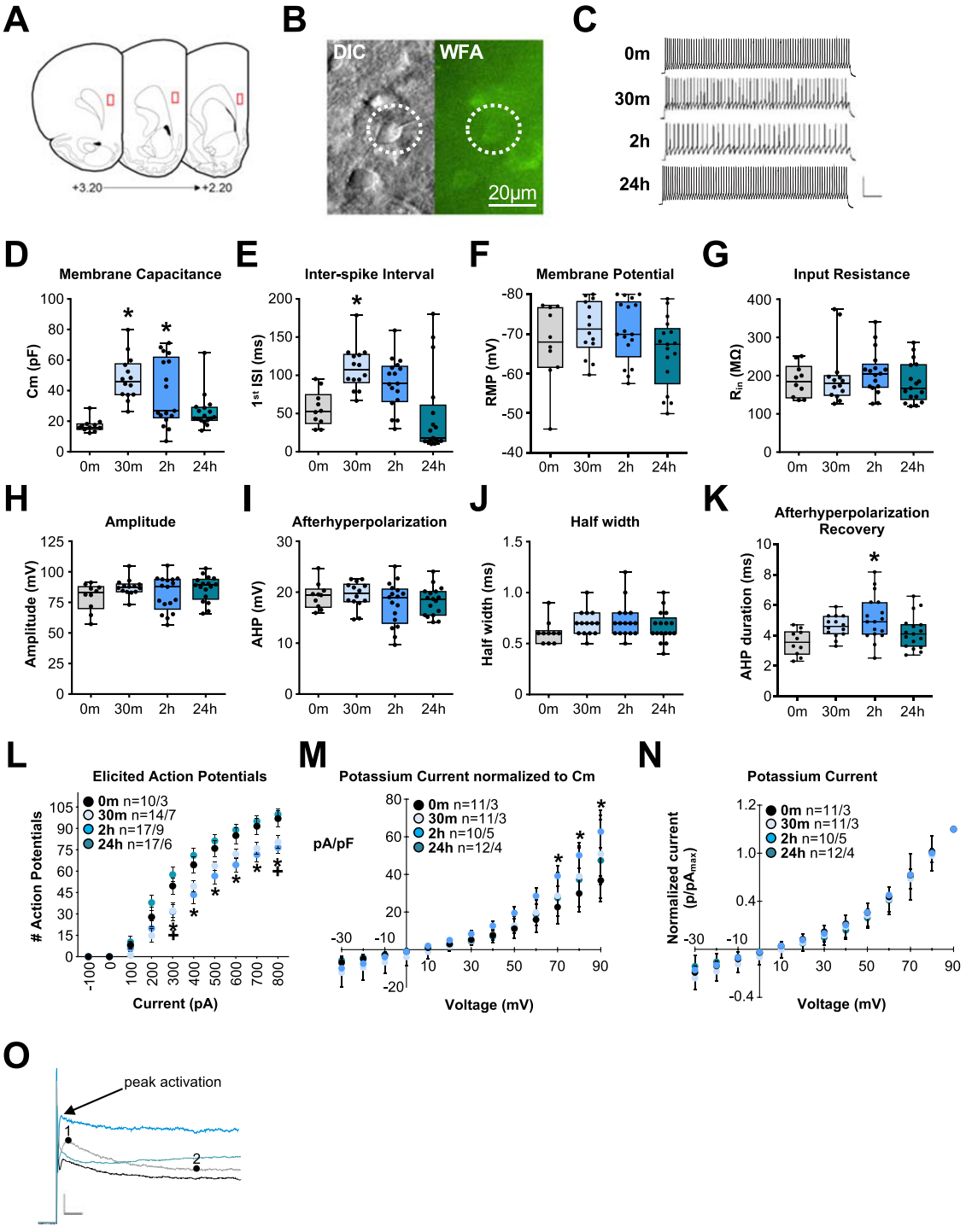

FIGURE 3 Cocaine-CPP memory reactivation alters the firing rate and potassium currents of PNN surrounded FSIs within the PL mPFC. (A) Schematic of coronal brain sections through PFC where recordings were performed, red boxes indicate recording regions; (B) DIC and WFA + images of a single cell recorded in PFC; (C) representative traces of action potentials evoked by 500 pA current injection for cells at different times after reactivation test. Scale bar represents 50 ms, 50 mV; (D) increased membrane capacitance of PNN surrounded FSIs 30 m and 2 h following cocaine memory reactivation; (E) increased duration of interspike interval 30 m after memory reactivation; (F) unaltered resting membrane potential; (G) input resistance; (H) amplitude; (I) after hyperpolarization potential; (J) half width; (K) increased AHP duration at 2 h; (L) average numbers of action potentials across range of current injections for different groups post reactivation, as well as control groups. * indicate significant reduction in action potentials at 30 m and + indicate significant reduction in action potentials at 2 h when compared with 0 m $p < 0.01$; (M) the effect of cocaine memory reactivation on potassium mediated current amplitudes was evaluated at different activation voltages by voltage-clamp recordings from PNN-surrounded parvalbumin FSIs and was increased 2 h when normalized to membrane capacitance; (N) no effect when normalized to maximum current; (O) representative traces of potassium mediated currents for each time point at +70 mV. Scale bar represents 200 pA, 10 ms

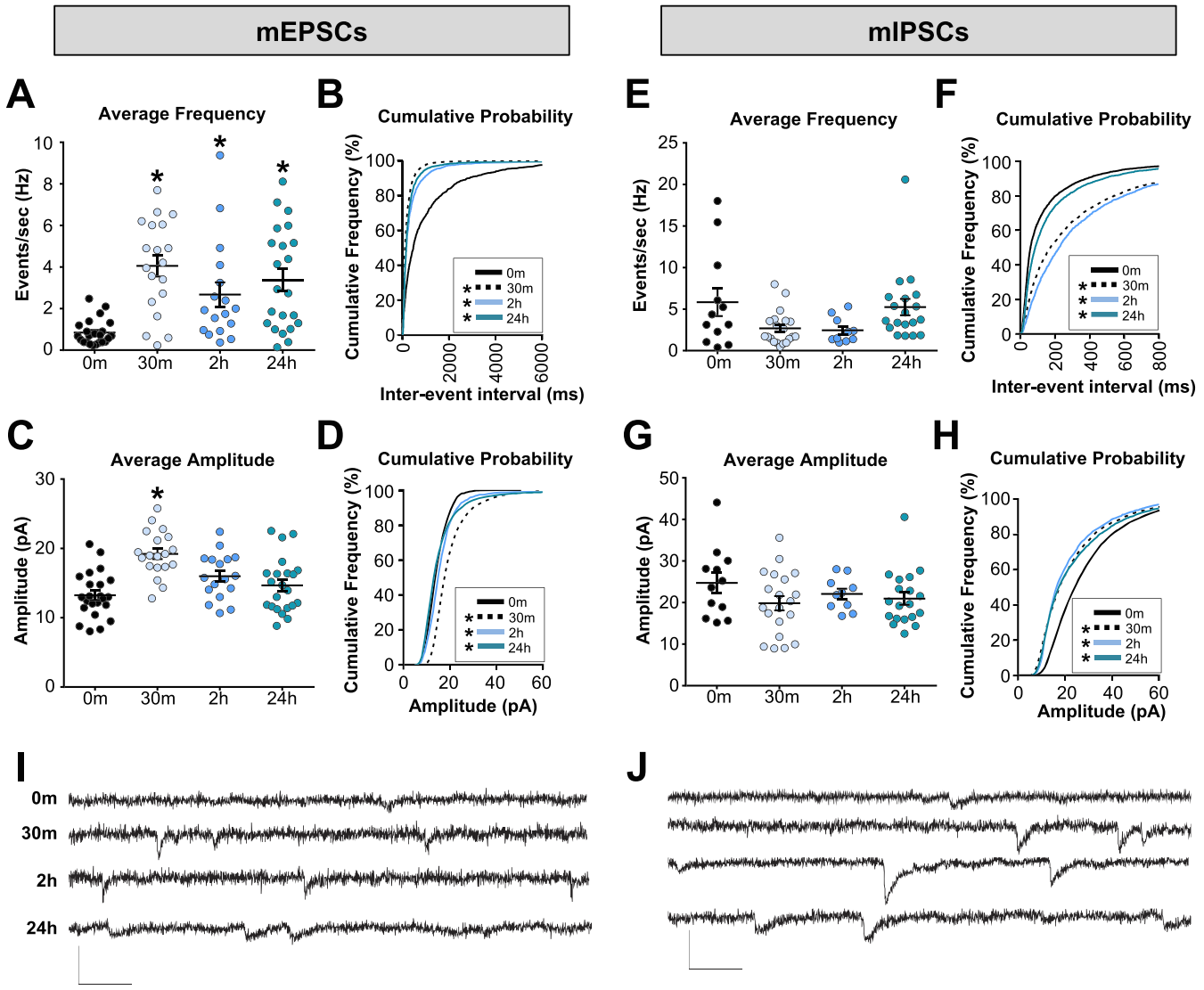

FIGURE 4 Cocaine-CPP memory reactivation increases mEPSC amplitude and frequency of PNN-surrounded FSIs within the PL PFC. (mEPSCs) cocaine-CPP memory reactivation significantly increased glutamatergic synaptic transmission. (A) Average frequency (Hz) of mEPSC events/neuron. *N*-sizes: (t = 0 [4]; t = 30 m [3]; t = 2 h [3]; t = 24 h [3]); $^{*}p < 0.05$, compared with t = 0 time point. (B) Cumulative probability of inter-event intervals for all events; $^{*}p < 0.001$; t = 0 compared with all time points. (C) Average amplitudes (pA) of mEPSC events/neuron; $^{*}p < 0.05$, compared with t = 0 time point; and (D) cumulative probability of amplitudes for all events (left); $^{*}p < 0.001$, t = 0 compared with all time points. (mIPSCs) cocaine-memory reactivation significantly altered cumulative distributions of inhibitory synaptic transmission. (E) Average frequency of mIPSCs events/neuron. *N*-sizes: (t = 0 [3]; t = 30 m [3]; t = 2 h [3]; t = 24 h [3]); (F) cumulative probability of inter-event intervals for all events (right); $^{*}p < 0.001$, t = 0 compared with all time points. (G) Average amplitudes of mIPSCs events/neuron and (H) cumulative probability of amplitudes for all events (right); $^{*}p < 0.001$, t = 0 compared with all time points. (I) Representative traces from mEPSCs; (J) representative traces from mIPSCs. Scale bar represents 50 pA, 500 μs

Additionally, we found differences in the cumulative distributions of both mEPSC inter-event intervals and amplitudes. Compared with t = 0, the inter-event intervals of all other time points shifted leftward, indicating that the inter-event interval was smaller (Figure 4B: $p < 0.01$; Kolmogorov-Smirnov D = 0.41), which indicates an increased frequency. There was also a potentiation of the mEPSC amplitude 30 min after memory reactivation compared with non-reactivated controls (Figure 4C; 0 min = 13.24 pA, 30 min = 19.21 pA, 2 h = 15.99 pA, and 24 h = 14.66 pA; $F_{3,77} = 10.97$, $p < 0.01$). In addition, there was a rightward shift in the cumulative distribution of individual amplitudes (Figure 4D: $p < 0.01$; Kolmogorov-Smirnov D = 0.35), indicating a potentiation in amplitudes at all time points when compared with t = 0. There were no significant differences in average mIPSC frequency (Figure 4E) or amplitude (Figure 4G). However, we did observe significant shifts in the cumulative distributions of the mIPSC inter-event intervals (Figure 4F: $p < 0.01$; Kolmogorov-Smirnov D = 0.29) and individual amplitudes (Figure 4H: $p < 0.01$; Kolmogorov-Smirnov D = 0.22); inter-event intervals shifted right from t = 0, where amplitudes shifted left from t = 0, indicative of a decrease in inhibitory synaptic transmission. In summary, these data

support our hypothesis that there is a decrease in FSI firing and an increase in the excitatory:inhibitory balance onto FSIs after cocaine CPP memory reactivation.

4 | DISCUSSION

This study is the first to examine functional changes in PNN-surrounded parvalbumin FSIs in the prelimbic mPFC after cocaine-associated memory reactivation. Our previous studies have shown that PNN degradation influences pyramidal neuron firing and attenuates cocaine reinstatement.[13] Our group and others have also demonstrated that PNNs and parvalbumin are susceptible to changes in intensity following cocaine exposure,[25]other drugs of abuse, high fat diets,[23,27] and sleep disruption.[31] Importantly, PNN-surrounded parvalbumin FSIs are heavily implicated and have been studied extensively in the field of learning and memory.[11,12,18,19] This work expands our previous findings[13] on the role of PNNs in cocaine-associated CPP memory and indicates that cocaine-associated memory reactivation alone alters the properties of PNN-surrounded parvalbumin FSIs.

Here, we found that cocaine memory reactivation reduced parvalbumin intensity following cocaine memory reactivation but did not change WFA intensity. This was unexpected, as PNNs and parvalbumin tend to change together and in the same direction, as often demonstrated in developmental studies,[37] schizophrenia,[38] and our own work with cocaine exposure.[25] However, there are exceptions. For example, Harkness and colleagues found that sleep disruption increased parvalbumin intensity while PNN intensity remained unchanged.[31] Furthermore, parvalbumin and PNN development within the hippocampus[39] do not coincide as they do in the cortex.[37] This shows that alterations in PNNs and parvalbumin are far more complex and could be differentially regulated by various stimuli and experiences in adulthood. The decrease in parvalbumin after cocaine memory reactivation may contribute to short-term plasticity to increase inhibition onto pyramidal neurons, since reducing parvalbumin concentrations increases synaptic facilitation.[40] Decreases in parvalbumin may also reduce gamma oscillations[41] that are important for cognition and working memory. The rapid decrease in parvalbumin (30 min after memory reactivation) may be associated with a rapid de-maturation state in which silent synapses are induced during the memory reconsolidation window,[42] but it remains to be determined whether this occurs in mPFC parvalbumin neurons. Interestingly, we also found small increases in parvalbumin cell axis diameter 2 and 24 h after cocaine memory reactivation. There exists an inverse relationship between parvalbumin levels and mitochondrial volume and cell morphology[43]; the lower parvalbumin levels are thus consistent with the increased diameter, but the functional consequences of this increase are presently unknown.

In addition to parvalbumin intensity changes, cocaine memory reactivation also induced functional adaptations of PNN-surrounded parvalbumin FSIs. Synaptically, there were increases in frequency and amplitude of mEPSC events (Figure 4A-D), indicating that there may be both pre- and post-synaptic increases in excitatory transmission following memory reactivation, when the memory is in a labile state.[3,5] Increases in excitatory transmission are commonly observed in cortical neurons during periods of learning and often result from decreased inhibitory input from nearby interneurons.[30,44] This decrease in PNN-surrounded parvalbumin FSI inhibition would likely alter the local microcircuit to increase pyramidal neuron activity within the mPFC and increase excitation to subcortical regions. In fact, we previously reported that PNN removal, which decreases FSI firing (unpublished data), potentiated pyramidal neuron firing.[44] Our observation of increased excitatory inputs to FSIs was corroborated by an increase in VGlut1 puncta and an overall decrease in the GAD/VGlut1 ratio on parvalbumin mPFC neurons (Figure 2D-E). Although intrinsic excitability returns to levels indistinguishable from controls at 24 h, excitatory tone remains elevated, and parvalbumin levels remain decreased, indicating that the changes last beyond the standard 6 h period when the window of memory reconsolidation closes.[3,5] The mEPSC and mIPSC findings support other studies that reported changes in excitatory but not inhibitory synaptic transmission onto parvalbumin FSIs after prolonged cocaine withdrawal.[44] The persistent decrease in parvalbumin staining intensity may alter the excitatory:inhibitory network in the mPFC, as parvalbumin and GAD levels are often highly correlated,[11] suggesting that cocaine memory reactivation may decrease GABA release to disinhibit pyramidal neuron firing. Interestingly, an increase in pyramidal firing appears to bidirectionally modulate the transcription of parvalbumin and GAD, with high levels of pyramidal firing producing a decrease in transcription of parvalbumin and GAD through a GluN2B-dependent pathway.[45]

To help determine underlying mechanisms for the decrease in elicited action potentials after cocaine memory reactivation (Figure 3L), we measured intrinsic properties of PNN-surrounded FSIs and found an increase in the interspike interval, membrane capacitance, and afterhyperpolarization recovery time (Figure 3D-E,K). Membrane capacitance is commonly used as an indicator of cell size, and this increase was validated by an increase in parvalbumin cell axis diameter when measured immunohistochemically (Figure 2F). Alterations in interspike interval, membrane capacitance, and afterhyperpolarization recovery are indicative of changes in potassium current that repolarizes or hyperpolarizes the cell, increasing the threshold for an action potential firing.[46,47] Indeed, our electrophysiological experiments confirmed that there is an overall increase in potassium current following cocaine memory reactivation. An increase in potassium current, when normalized to membrane capacitance, can be due to multiple factors, including an increase in surface channel expression, an increase in single channel conductance, or an increase in the probability of opening of the existing channels.[46,48] We speculate that a decrease in excitability, paired with an increase in potassium current, points in the direction of muscarinic (m-type) potassium channels as mediating this change in parvalbumin neuron firing. M-type potassium channels maintain the resting membrane potential and are activated during hyperpolarization.[49] Importantly, m-type channels are also involved in learning and memory.[50] Blockade of m-type

potassium channels within the infralimbic PFC decrease fear expression and initiate fear extinction.[50] This prior study also found an increase in excitability after blocking m-type channels, which aligns with predicted adaptations of m-type channel transmission following cocaine memory reactivation. Future experiments will examine the role of m-type channels in cocaine-associated memories.

In conclusion, we show that cocaine-associated memory reactivation reduces excitation of PNN-surrounded parvalbumin FSIs by increasing the potassium (hyperpolarizing) current. These experiments provide a novel mechanism for plasticity in PNN-surrounded parvalbumin FSIs involved in the reactivation of cocaine-associated memories. Future experiments will determine which potassium channels are increasing in surface expression or conductance, ultimately contributing to the functional changes within cortical PNN surrounded parvalbumin FSIs to promote cocaine-seeking behaviors.

ACKNOWLEDGEMENTS

The authors thank Dr. Karen Mruk (University of Wyoming) and Dr. Brian Lee (Allen Institute for Brain Research) for their expertise and guidance throughout electrophysiology experiments. We also thank Dr. Paige Dingess, Georgia Kirkpatrick, and Maha Paracha for their support of this research. This work was supported by the National Institute on Drug Abuse R01 DA040965 (T.E.B., B.A.S., and S.A.A.), the National Institutes of Health Centers Program Grant P30 GM103398-32128 (T.E.B.), National Institute of Neurological Disorders and Stroke P30 NS061800 (S.A.A.), the Wyoming Scholars Program (D.J.B.), and the University of Wyoming Science Initiative (D.J.B.).

DISCLOSURE/CONFLICT OF INTEREST

The authors declare that there are no conflicts of interest.

AUTHORS CONTRIBUTION

TEB and BAS were responsible for the study concept and design. ETJ, JHH, AEG, DJB, and JAA contributed to the acquisition of animal behavior. ETJ drafted the manuscript, performed all electrophysiology, analyzed, and interpreted electrophysiological data. JHH and AEG performed immunohistochemical procedures, collected, and analyzed images. DMH performed all puncta data collection and analysis. TEB, BAS, SAA, and AT provided critical revision of the manuscript. All authors critically reviewed and approved final version for publication.

ORCID

Travis E. Brown https://orcid.org/0000-0003-2228-3219

REFERENCES

1. Milton AL, Everitt BJ. The psychological and neurochemical mechanisms of drug memory reconsolidation: implications for the treatment of addiction. *Eur J Neurosci*. 2010;31(12):2308-2319.
2. Tronson NC, Taylor JR. Addiction: a drug-induced disorder of memory reconsolidation. *Curr Opin Neurobiol*. 2013;23(4):573-580.
3. Nader K, Schafe GE, LeDoux JE. The labile nature of consolidation theory. *Nat Rev Neurosci*. 2000;1(3):216-219.
4. Lee JLC, Milton AL, Everitt BJ. Cue-induced cocaine seeking and relapse are reduced by disruption of drug memory reconsolidation. *J Neurosci*. 2006;26(22):5881-5887.
5. Sorg BA. Reconsolidation of drug memories. *Neurosci Biobehav Rev*. 2012;36(5):1400-1417.
6. Xue Y-X, Luo YX, Wu P, et al. A memory retrieval-extinction procedure to prevent drug craving and relapse. *Science*. 2012;336(6078):241-245.
7. Celio M, Calbindin R. D-28k and parvalbumin in the rat nervous system. *Neuroscience*. 1990;35(2):375-475.
8. Lee AT, Gee SM, Vogt D, Patel T, Rubenstein JL, Sohal VS. Pyramidal neurons in prefrontal cortex receive subtype-specific forms of excitation and inhibition. *Neuron*. 2014;81(1):61-68.
9. Cabungcal J-H, Steullet P, Kraftsik R, Cuenod M, Do KQ. A developmental redox dysregulation leads to spatio-temporal deficit of parvalbumin neuron circuitry in a schizophrenia mouse model. *Schizophr Res*. 2019;213:96-106.
10. Volk DW, Edelson JR, Lewis DA. Altered expression of developmental regulators of parvalbumin and somatostatin neurons in the prefrontal cortex in schizophrenia. *Schizophr Res*. 2016;177(1-3):3-9.
11. Donato F, Rompani SB, Caroni P. Parvalbumin-expressing basket-cell network plasticity induced by experience regulates adult learning. *Nature*. 2013;504(7479):272-276.
12. Korotkova T, Fuchs EC, Ponomarenko A, von Engelhardt J, Monyer H. NMDA receptor ablation on parvalbumin-positive interneurons impairs hippocampal synchrony, spatial representations, and working memory. *Neuron*. 2010;68(3):557-569.
13. Slaker M, Churchill L, Todd RP, et al. Removal of perineuronal nets in the medial prefrontal cortex impairs the acquisition and reconsolidation of a cocaine-induced conditioned place preference memory. *J Neurosci*. 2015;35(10):4190-4202.
14. Kwok JCF, Carulli D, Fawcett JW. In vitro modeling of perineuronal nets: hyaluronan synthase and link protein are necessary for their formation and integrity. *J Neurochem*. 2010;114(5):1447-1459.
15. Morris NP, Henderson Z. Perineuronal nets ensheath fast spiking, parvalbumin-immunoreactive neurons in the medial septum/diagonal band complex. *Eur J Neurosci*. 2000;12(3):828-838.
16. Cabungcal J-H, Steullet P, Morishita H, et al. Perineuronal nets protect fast-spiking interneurons against oxidative stress. *Proc National Acad Sci*. 2013;110(22):9130-9135.
17. Carulli D, Pizzorusso T, Kwok JCF, et al. Animals lacking link protein have attenuated perineuronal nets and persistent plasticity. *Brain*. 2010;133(8):2331-2347.
18. Morikawa S, Ikegaya Y, Narita M, Tamura H. Activation of perineuronal net-expressing excitatory neurons during associative memory encoding and retrieval. *Sci Rep-Uk*. 2017;7(1):1-9.
19. Yang S, Cacquevel M, Saksida LM, et al. Perineuronal net digestion with chondroitinase restores memory in mice with tau pathology. *Exp Neurol*. 2015;265:48-58.
20. Gogolla N, Caroni P, Lüthi A, Herry C. Perineuronal nets protect fear memories from erasure. *Science*. 2009;325(5945):1258-1261.
21. Hylin MJ, Orsi SA, Moore AN, Dash PK. Disruption of the perineuronal net in the hippocampus or medial prefrontal cortex impairs fear conditioning. *Learn Memory*. 2013;20(5):267-273.
22. Thompson EH, Lensjø KK, Wigestrand MB, Malthe-Sørenssen A, Hafting T, Fyhn M. Removal of perineuronal nets disrupts recall of a remote fear memory. *Proc National Acad Sci*. 2018;115(3):607-612.
23. Dingess PM, Harkness JH, Slaker M, et al. Consumption of a high-fat diet alters Perineuronal nets in the prefrontal cortex. *Neural Plast*. 2018;2018(2108373):1-8.
24. Reichelt AC, Hare DJ, Bussey TJ, Saksida LM. Perineuronal nets: plasticity, protection, and therapeutic potential. *Trends Neurosci*. 2019;42(7):458-470.
25. Slaker ML, Jorgensen ET, Hegarty DM, et al. Cocaine exposure modulates perineuronal nets and synaptic excitability of fast-spiking

interneurons in the medial prefrontal cortex. *Eneuro*. 2018;5, ENEURO.0221–18.2018(5).
26. Blacktop JM, Todd RP, Sorg BA. Role of perineuronal nets in the anterior dorsal lateral hypothalamic area in the acquisition of cocaine-induced conditioned place preference and self-administration. *Neuropharmacology*. 2017;118:124-136.
27. Lasek AW, Chen H, Chen W-Y. Releasing addiction memories trapped in perineuronal nets. *Trends Genet*. 2017;34:197-208.
28. Tewari BP, Chaunsali L, Campbell SL, Patel DC, Goode AE, Sontheimer H. Perineuronal nets decrease membrane capacitance of peritumoral fast spiking interneurons in a model of epilepsy. *Nat Commun*. 2018;9(1):4724.
29. Balmer TS. Perineuronal nets enhance the excitability of fast-spiking neurons. *Eneuro*. 2016;3, ENEURO.0112–16.2016(4).
30. Froemke RC. Plasticity of cortical excitatory-inhibitory balance. *Annu Rev Neurosci*. 2015;38(1):195-219.
31. Harkness JH, Bushana PN, Todd RP, Clegern WC, Sorg BA, Wisor JP. Sleep disruption elevates oxidative stress in parvalbumin-positive cells of the rat cerebral cortex. *Sleep*. 2018;42:1-15.
32. Slaker ML, Harkness JH, Sorg BA. A standardized and automated method of perineuronal net analysis using *Wisteria floribunda* agglutinin staining intensity. *Ibro Reports*. 2016;1:54-60.
33. Hegarty DM, Hermes SM, Largent-Milnes TM, Aicher SA. Capsaicin-responsive corneal afferents do not contain TRPV1 at their central terminals in trigeminal nucleus caudalis in rats. *J Chem Neuroanat*. 2014;61:1-12.
34. Hegarty DM, Tonsfeldt K, Hermes SM, Helfand H, Aicher SA. Differential localization of vesicular glutamate transporters and peptides in corneal afferents to trigeminal nucleus caudalis. *J Comp Neurol*. 2010;518(17):3557-3569.
35. Paxinos G, Watson C. *The Rat Brain in Stereotaxic Coordinates*; 1982:13-153.
36. Baranauskas G, Tkatch T, Nagata K, Yeh JZ, Surmeier DJ. Kv3.4 subunits enhance the repolarizing efficiency of Kv3.1 channels in fast-spiking neurons. *Nat Neurosci*. 2003;6(3):258-266.
37. Ueno H, Suemitsu S, Okamoto M, Matsumoto Y, Ishihara T. Parvalbumin neurons and perineuronal nets in the mouse prefrontal cortex. *Neuroscience*. 2017;343:115-127.
38. Enwright JF, Sanapala S, Foglio A, Berry R, Fish KN, Lewis DA. Reduced labeling of parvalbumin neurons and perineuronal nets in the dorsolateral prefrontal cortex of subjects with schizophrenia. *Neuropsychopharmacol Official Publ am Coll Neuropsychopharmacol*. 2016;41(9):2206-2214.
39. Yamada J, Jinno S. Spatio-temporal differences in perineuronal net expression in the mouse hippocampus, with reference to parvalbumin. *Neuroscience*. 2013;253:368-379.
40. Caillard O, Moreno H, Schwaller B, Llano I, Celio MR, Marty A. Role of the calcium-binding protein parvalbumin in short-term synaptic plasticity. *Proc National Acad Sci*. 2000;97(24):13372-13377.
41. Volman V, Behrens MM, Sejnowski TJ. Downregulation of parvalbumin at cortical GABA synapses reduces network gamma oscillatory activity. *J Neurosci Official J Soc Neurosci*. 2011;31(49):18137-18148.
42. Wright WJ, Graziane NM, Neumann PA, et al. Silent synapses dictate cocaine memory destabilization and reconsolidation. *Nat Neurosci*. 2019;23:32-46.
43. Lichvarova L, Henzi T, Safiulina D, Kaasik A, Schwaller B. Parvalbumin alters mitochondrial dynamics and affects cell morphology. *Cell Mol Life Sci*. 2018;75(24):4643-4666.
44. Campanac E, Hoffman DA. Repeated cocaine exposure increases fast-spiking interneuron excitability in the rat medial prefrontal cortex. *J Neurophysiol*. 2013;109(11):2781-2792.
45. Parrish RR, Codadu NJ, Racca C, Trevelyan AJ. Pyramidal cell activity levels affect the polarity of gene transciption changes in interneurons. *J Neurophysiol*. 2018;120(5):2358-2367.
46. Hodgkin AL, Huxley AF. A quantitative description of membrane current and its application to conduction and excitation in nerve. *J Physiology*. 1952;117(4):500-544.
47. Bean BP. The action potential in mammalian central neurons. *Nat Rev Neurosci*. 2007;8(6):451-465.
48. Schwake M, Pusch M, Kharkovets T, Jentsch TJ. Surface expression and single channel properties of KCNQ2/KCNQ3, M-type K^+ channels involved in epilepsy. *J Biol Chem*. 2000;275(18):13343-13348.
49. Brown DA, Passmore GM. Neural KCNQ (Kv7) channels. *Brit J Pharmacol*. 2009;156(8):1185-1195.
50. Santini E, Porter JT. M-type potassium channels modulate the intrinsic excitability of infralimbic neurons and regulate fear expression and extinction. *J Neurosci Official J Soc Neurosci*. 2010;30(37):12379-12386.

How to cite this article: Jorgensen ET, Gonzalez AE, Harkness JH, et al. Cocaine memory reactivation induces functional adaptations within parvalbumin interneurons in the rat medial prefrontal cortex. *Addiction Biology*. 2020;e12947. https://doi.org/10.1111/adb.12947